

## RESEARCH PAPER

# Extra-virgin olive oil ameliorates cognition and neuropathology of the 3xTg mice: role of autophagy

Elisabetta Laurettil<sup>1</sup>, Luigi Iuliano<sup>2</sup> & Domenico Praticò<sup>1</sup><sup>1</sup>Department of Pharmacology and Center for Translational Medicine, Lewis Katz School of Medicine, Temple University, Philadelphia, Pennsylvania, 19140<sup>2</sup>Department of Medical Sciences and Biotechnology, Sapienza University of Roma, Latina 04100, Italy

## Correspondence

Domenico Praticò, 947, Medical Education and Research Building, 3500 North Broad Street, Philadelphia, PA 19140.

Tel: 215 707 9380; Fax: 215 707 9890;

E-mail: praticod@temple.edu

## Funding Information

This work presented in this paper was in part supported by a grant from the Wanda Simone Endowment for Neuroscience.

Received: 17 March 2017; Revised: 1 May 2017; Accepted: 22 May 2017

doi: 10.1002/acn3.431

## Abstract

**Objective:** Consumption of extra virgin olive oil (EVOO), a major component of the Mediterranean diet, has been associated with reduced incidence of Alzheimer's disease (AD). However, the mechanisms involved in this protective action remain to be fully elucidated. **Methods:** Herein, we investigated the effect of daily consumption of EVOO on the AD-like phenotype of a mouse model of the disease with plaques and tangles. **Results:** Triple transgenic mice (3xTg) received either regular chow or a chow diet supplemented with EVOO starting at 6 months of age for 6 months, then assessed for the effect of the diet on the AD-like neuropathology and behavioral changes. Compared with controls, mice receiving the EVOO-rich diet had an amelioration of their behavioral deficits, and a significant increase in the steady state levels of synaptophysin, a protein marker of synaptic integrity. In addition, they had a significant reduction in insoluble A $\beta$  peptide levels and deposition, lower amount of phosphorylated tau protein at specific epitopes, which were secondary to an activation of cell autophagy. **Interpretation:** Taken together, our findings support a beneficial effect of EVOO consumption on all major features of the AD phenotype (behavioral deficits, synaptic pathology, A $\beta$  and tau neuropathology), and demonstrate that autophagy activation is the mechanism underlying these biological actions.

## Introduction

Alzheimer's disease (AD) is an irreversible, age-associated neurodegenerative disorder characterized by progressive memory loss and cognitive decline, and the leading cause of dementia accounting for 5 million cases in the US and 44 million cases worldwide. In 2015, AD cost was over 200 billion dollars in the US alone, and over 600 billion dollars worldwide.<sup>1</sup> Only approximately 5% of the total AD cases are due to genetic mutations responsible for abnormal Amyloid-beta (A $\beta$ ) elevation and deposition in the brain. However, the etiology for the sporadic form of AD accounting for 95% of the remaining cases is still unknown, and so far no effective therapy is available.<sup>2</sup> As result, in recent years the AD research field has moved more and more toward prevention and away from treatment. Today, we know that delaying the onset of AD by even 1 year could significantly reduce new diagnosed

cases, and that implementing efficient preventative measures could ultimately result in significant annual savings for the skyrocketing costs related to the disease worldwide.<sup>3</sup> For this reason, it is extremely important to identify new targets and tools that by acting as preventative strategies could potentially offer novel therapeutic opportunities with the capacity not only to prevent but also halt the disease progression.

Epidemiological and clinical studies have consistently indicated that higher adherence to the Mediterranean diet is associated with a reduced risk of developing mild cognitive impairment and AD, and a reduced risk of progressing from mild cognitive impairment to AD.<sup>4,5</sup> Among the different nutrients that characterize the Mediterranean diet, a lot of attention has been focused on the extra-virgin olive oil (EVOO) daily intake, which is estimated to be quite high in the Mediterranean area populations compared with other geographical regions around the world.<sup>6,7</sup>

Previous studies have shown that consumption of EVOO results in amelioration of learning and memory in SAMP8 mice, and a reversal of age-related dysfunctions in old mice.<sup>8–10</sup> In both cases, the authors attributed those beneficial effects to the EVOO phenolic compounds and their antioxidant ability to protect against the disease-related and age-associated brain oxidation of these animals.<sup>8–10</sup> More recently, it was shown that EVOO administration to a transgenic mouse model of AD-like brain amyloidosis, TgSwDI, reduces parenchymal and vascular A $\beta$  levels via an enhancement of its clearance.<sup>11</sup>

However, because this mouse model manifests only one of the two main aspects of the AD phenotype, the effect of EVOO on tau neuropathology remains to be fully investigated. With this goal in mind, in the present paper we evaluated the biological effect of EVOO in the triple transgenic mice (3xTg), which are known to develop both amyloid plaques and neurofibrillary tangles.<sup>12</sup>

## Methods and Materials

### Animals and treatment

All animal procedures were approved by the Institutional Animal Care and Usage Committee, in accordance with the US National Institutes of Health guidelines. The 3xTg mice harboring 3 transgenes (PS1<sub>M146V</sub>, tau<sub>P301L</sub>, and APP<sub>Swe</sub>) were used in this study.<sup>12</sup> Animals were kept in a pathogen-free environment, on a 12-h light/dark cycle and fed a normal chow and water ad libitum. Male and female mice were used throughout the studies. Starting at 6 months of age, mice were randomized into two groups: one fed with standard diet (CTR,  $n = 12$ ), the other with EVOO-enriched diet (EVOO,  $n = 10$ ) for 6 months. The EVOO was from the olive growing area of Apulia region (Torremaggiore, Foggia, Italy). Olive fruits from the cultivar “Peranzana” were processed immediately after harvesting and EVOO obtained by crushing the olives under mechanical cold pressure to preserve all the nutritional components, and meet the stringent criteria of the premium quality level (free acid content < 0.3 g%, peroxide value < 7 mEq/Kg, K232 < 1.85). Fresh diet was provided every other day. During the treatment, body weight of the animals was measured every 30 days to ascertain that the EVOO diet did not affect caloric intake. Mice underwent the same behavioral tests at 6 (for baseline assessment), 9 (3 months treatment) and 12 months (6 months treatment) of age as described below and then euthanized at the last time point. After perfusion brains were removed, gently rinsed in cold 0.9% phosphate-buffered saline and immediately dissected in two halves. One half was immediately stored at  $-80^{\circ}\text{C}$  for biochemistry;

the other half was fixed in 4% paraformaldehyde in phosphate-buffered saline, pH7.4 for immunohistochemistry studies.

### Behavioral tests

All the animals were handled for at least 3–4 consecutive days before testing and all tests were conducted by an experimenter unaware of the treatment.

#### Y-maze

The Y-maze apparatus consisted of 3 arms, 32 cm (long) 610 cm (wide) with 26-cm walls (San Diego Instruments, San Diego, CA). As previously described<sup>13,14</sup>, testing was always performed in the same room and at the same time to ensure environmental consistency as previously described. After introduction to the center of the Y-maze, the animal is allowed to freely explore the three arms for 5 min and the sequence and total number of arms entered was video-recorded in order to calculate the percentage of alternation. Any entry into an arm was considered valid if all limbs were within the arm. An alternation was defined as three consecutive entries in three different arms (1,2,3 or 2,3,1, etc.). The percentage alternation score was calculated using the following formula: total alternation number/total number of entries–2)  $\times 100$ .

#### Fear conditioning

The fear conditioning test was performed in a conditioning chamber (19  $\times$  25  $\times$  19 cm) equipped with black methacrylate walls, transparent front door, a speaker, and grid floor (Start Fear System; Harvard Apparatus) as previously described.<sup>13</sup> During the first day of the test, mice were placed into the conditioning chamber and allowed free exploration for 2 min in the white noise (65 dB) before the delivery of the conditioned stimulus (CS) tone (30 sec, 90 Db, 2000 Hz) paired with a foot-shock unconditioned stimulus (2 sec, 0.6 mA) through a grid floor at the end of the tone. In the training phase, each mouse received a total of three CS tones paired with a 30-sec inter trial interval. At the end of the training phase, the mouse was removed from the chamber and placed back in its home cage. 24 h after, in the contextual fear conditioning stage, the animal was returned to the same environment for 5 min in the presence of white noise only (65 dB). The animal's freezing responses to the environmental context were recorded. The cue fear conditioning stage started 2 h after the contextual stage. The animal was placed back into the chamber after providing different contextual cues, such as white wall, smooth

metal floor, lemon extract drops, and red light condition. After 3 min of free exploration, the mouse was exposed to the exactly same 3 CS tones with 30 sec inter trial interval in the training stage without the foot-shock. The freezing score for each mouse was recorded.

### Morris water maze

The apparatus used to perform the Morris water maze task consists of a large circular pool (122 cm in diameter) with walls 76 cm high, which is filled with water maintained at  $22^{\circ}\pm 2^{\circ}\text{C}$ , and made opaque by the addition of a nontoxic white paint. Mice were given four daily trials for four consecutive days. Animals were trained to swim to a submerged Plexiglas platform starting each time from different positions. If they fail to find the platform within 60 sec, they were manually guided to the platform and allowed to remain there for 15 sec. Mice were trained to reach the hidden platform within 20 sec (escape latency). On the fifth day, during the probe, mice were allowed to swim in the pool without the platform for 60 sec, and the number of entries in the platform zone and the time spent in the different quadrants were recorded. During subsequent trials the swimming speed was also determined.<sup>14</sup>

### Immunoblot analyses

Immunoblot analyses were performed as previously described<sup>15,16</sup>. Briefly, proteins were extracted in enzyme immunoassay buffer containing 250 mmol/L Tris base, 750 mmol/L NaCl, 5% NP-40, 25 mmol/L EDTA, 2.5% sodium deoxycholate, 0.5% sodium dodecyl sulfate, and an EDTA-free protease and phosphatase inhibitors cocktail tablet (Roche Applied Science, Indianapolis, IN, USA), sonicated, centrifuged at 56,700 g for 45 min at  $4^{\circ}\text{C}$ , and supernatants used for immunoblot analysis, as previously described. Total protein concentration was determined by using BCA Protein Assay Kit (Pierce, Rockford, IL). Samples were electrophoretically separated using 10% Bis-Tris gels or 3–8% Tris-acetate gel (Bio-Rad, Richmond, CA), according to the molecular weight of the target molecule, and then transferred onto nitrocellulose membranes (Bio-Rad). They were blocked with Odyssey blocking buffer for 1 h; and then incubated with primary antibodies overnight at  $4^{\circ}\text{C}$ . After three washing cycles with T-TBS, membranes were incubated with IRDye 800CW or IRDye 680CW-labeled secondary antibodies (LI-COR Bioscience, NE) at  $22^{\circ}\text{C}$  for 1 h. Signals were developed with Odyssey Infrared Imaging Systems (LI-COR Bioscience). Primary antibodies used in this paper are summarized in Table 1. Actin was always used as an internal loading control.

### Biochemical analysis

Mouse brain homogenates were sequentially extracted first in RIPA buffer for the soluble and then in formic acid (FA) for the insoluble protein fraction as previously described<sup>15,16</sup>. A $\beta$ 1-40 and A $\beta$ 1-42 levels were assayed by a sensitive sandwich ELISA kits (WAKO Chem., Richmond, VA).

### Immunohistochemistry

Primary antibodies used in this study are listed in Table 1. Immunostaining was performed as reported previously.<sup>13–16</sup> Briefly, serial 6- $\mu\text{m}$  thick coronal sections were mounted on 3-aminopropyl triethoxysilane-coated slides. Every eighth section from the habenular to the posterior commissure (8–10 sections per animal) was examined using unbiased stereological principles. The sections for A $\beta$  were deparaffinized, hydrated, pretreated with formic acid (FA; 88%) and subsequently with 3% hydrogen peroxide in methanol. The sections for tau were deparaffinized, hydrated, treated with 3% H<sub>2</sub>O<sub>2</sub> in methanol and citrate (10 mmol/L) for antigen retrieval. Sections were blocked in 2% fetal bovine serum and incubated with primary antibody for total tau (HT-7), phospho-tau (PHF-13, AT8), synaptophysin (SYP), microglia (Iba1) and A $\beta$  (4G8) overnight at  $4^{\circ}\text{C}$ . The following day, sections were incubated with biotinylated anti-mouse immunoglobulin G (Vector Laboratories, Burlingame, CA) and then developed by using the avidin-biotin complex method (Vector Laboratories) with 3,3'-diaminobenzidine as a chromogen. Consecutive sections were incubated in the absence of primary antibodies to ensure specificity of staining.

### Data analysis

Unpaired Student's *t*-test (two-sided) and one-way ANOVA were performed using Prism 5.0 (GraphPad Software, La Jolla, CA). All data are presented as mean  $\pm$  SEM. Significance was set at  $P < 0.05$ .

## Results

### Effect of EVOO-rich diet on animal weight

During the 6-months treatment, mice that received EVOO-enriched diet grew from an initial average weight of  $27.48 \pm 2.44$  gr to  $35.48 \pm 4.22$  gr. On the other hand, animals on a regular chow grew from an average weight of  $26.9 \pm 3.87$  to  $31.88 \pm 3.77$ . Overall, we did not observe any statistically significant difference between the two groups of mice during the study, except for the

**Table 1.** Antibodies used in the study.

Antibody	Immunogen	Host	Application	Source	Catalog number
4G8	aa 18-22 of human beta amyloid (VFFAE)	Mouse	IHC	Covance	SIG-39220
APP	aa 66-81 of APP {N-terminus}	Mouse	WB	Millipore	MAB348
BACE1	aa human BACE (CLRQHQHDDFADDISLLK)	Rabbit	WB	IBL	18711
ADAM10	aa 732-748 of human ADAM 10	Rabbit	WB	Millipore	AB19026
PS-1	aa around valine 293 of human presenilin 1	Rabbit	WB	Cell Signaling	3622S
Nicastrin	aa carboxy-terminus of human Nicastrin	Rabbit	WB	Cell Signaling	3632
APH-1	Synthetic peptide from hAPH-1a	Rabbit	WB	Millipore	AB9214
Pen-2	aa N-terminal of human and mouse Pen-2	Rabbit	WB	Invitrogen	36-7100
APP-C99	Recombinant protein corresponding to Human APP-C99	Mouse	WB	Millipore	MABN380
HT-7	aa 159-163 of human tau	Mouse	WB, IHC	Thermo	MN1000
AT-8	Peptide containing phospho-S202/T205	Mouse	WB, IHC	Thermo	MN1020
AT-180	Peptide containing phospho-T231/S235	Mouse	WB	Thermo	P10636
AT-270	Peptide containing phospho-T181	Mouse	WB	Thermo Scientific	MN1050
PHF-13	Peptide containing phospho-Ser396	Mouse	WB, IHC	Cell Signaling	9632
CDK5	Peptide mapping the C-term of human CDK5	Rabbit	WB	Santa Cruz	sc-173
P35/25	aa mapping to C-term of P35	Rabbit	WB	Santa Cruz	sc-820
PP2A	aa corresponding to C-term of PP2A	Rabbit	WB	Thermo Scientific	PA5-17510
P38	aa of human p38 MAPK	Rabbit	WB	Cell Signaling	9212
pP38	aa around Thr180/182 of human p38 MAPK	Rabbit	WB	Cell Signaling	4511
PSD95	Purified recombinant rat PSD-95	Mouse	WB	Thermo	MA1-045
SYP	aa 221-313 of SYP of human origin	Mouse	WB, IHC	Santa Cruz	sc-55507
IBA1	Linear peptide corresponding to human IBA1	Mouse	WB, IHC	Millipore	MABN92
GFAP	spinal chord homogenate of bovine origin	Mouse	WB	Santa Cruz	sc-33673
ATG5/12	KLH-conjugated linear peptide corresponding to human ATG5	Rabbit	WB	Millipore	ABC14
ATG7	Synthetic peptide corresponding to N-term of ATG7	Rabbit	WB	Cell Signaling	2631
LC3	Synthetic peptide corresponding to N-term of LC3	Rabbit	WB	Cell Signaling	2775
CD10	aa 230-550 mapping within an internal region of CD10 of human origin	Rabbit	WB	Santa Cruz	sc-9149
IDE	Synthetic peptide corresponding to N-term of human IDE	Goat	WB	Santa Cruz	sc-27265
ApoE	19-311 mapping at the C-terminus of apoE of mouse origin	Rabbit	WB	Santa Cruz	sc-98574
CREB	Synthetic peptide corresponding to N-term of human CREB	Rabbit	WB	Cell Signaling	9197
pCREB	Synthetic peptide corresponding to the residues surrounding Ser133 of CREB	Rabbit	WB	Cell Signaling	9198
C-Fos	Peptide mapping the internal region of human c-Fos	Rabbit	WB	Santa Cruz	sc-253
BDNF	Peptide mapping the internal region of human BDNF	Rabbit	WB	Santa Cruz	sc-456
Actin	gizzard Actin of avian origin	Mouse	WB	Santa Cruz	sc-47778

WB, Western blot; IHC, immunohistochemistry.

10 month time-point when the treated mice had a higher body weight than untreated one (Fig. 1A).

### **EVOO-rich diet restores working and spatial memory in 3xTg mice**

To determine the effect of EVOO-rich diet on behavior, animals were initially tested at 6 months to establish their behavioral baseline performance. Mice were tested again in the same tasks after 3 and 6 months on the EVOO-rich diet, at age of 9 and 12 months respectively. As shown in Figure 1B, in the Y-maze, compared with baseline (6 months), the mice at 9 and 12 months showed a reduction in the number of entries that reached the statistical significance for the CTR group at 9 months. When we

assessed the percentage of alternation, as expected, we observed a reduction of this parameter in the CTR group at both 9 and 12 months but, this was completely rescued in the EVOO treated mice (Fig. 1B). Next, mice underwent fear conditioning testing. No differences were observed in the freezing time during the training session (not shown) and during the contextual recall of the EVOO mice compared with their controls in both time points (Fig. 1C). Compared to control, the EVOO group had an increased freezing response activity in the cued recall phase, but the difference did not reach statistical significance (Fig. 1C). Finally, animals were tested in the Morris water-maze paradigm. All mice in each group were able to reach the training criterion within 4 days and no differences were found during the training session (not shown).

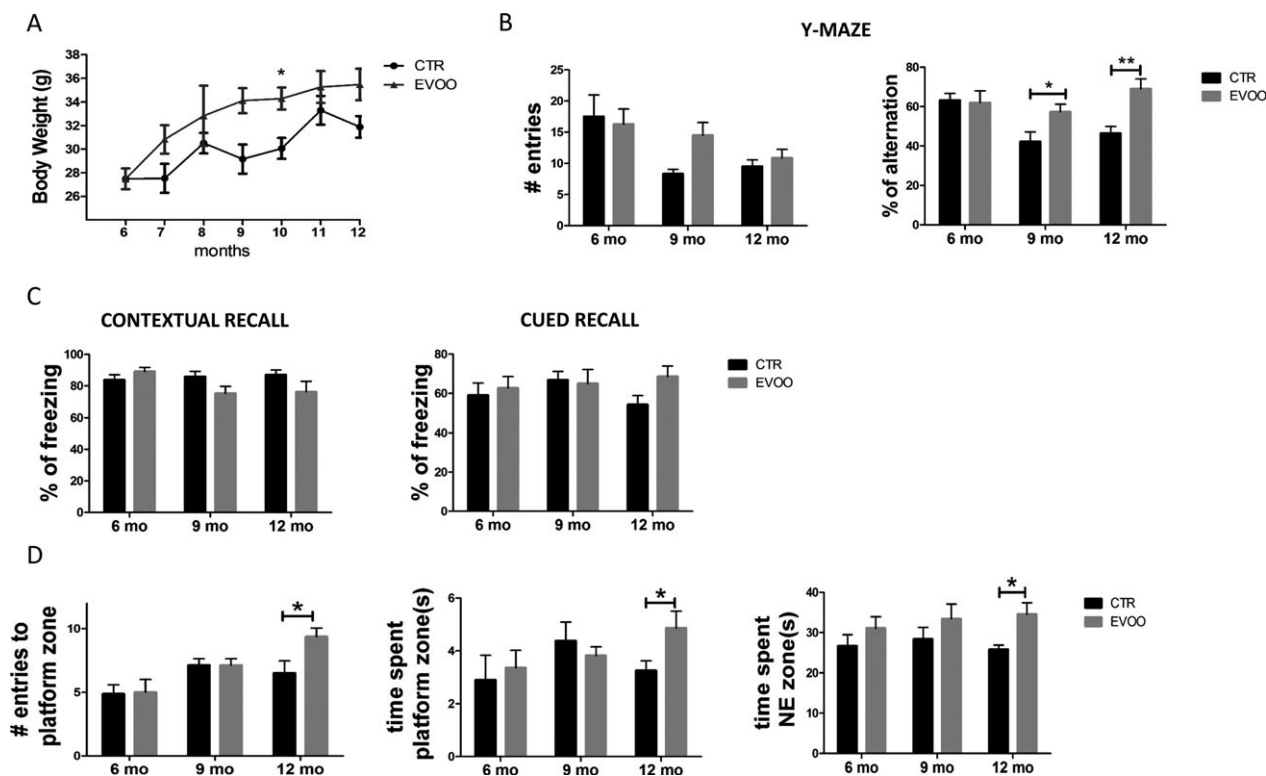


**Figure 1.** Chronic administration of EVOO-rich diet ameliorates behavioral impairments in 3xTg mice. Starting at 6 months of age, 3xTg mice were randomized to receive regular chow diet (CTR) or diet enriched with EVOO (EVOO) until they were 12-month-old. (A) Monthly body weight of CTR ( $n = 12$ ) and EVOO ( $n = 10$ ) mice from the beginning until the end of the study. (B) The same mice were tested in the Y-maze paradigm for the number of entries and the percentage of alternation ( $*P < 0.05$ ,  $**P < 0.01$ ). (C) Percentage of freezing in the contextual and cued phase of the fear conditioning paradigm (CTR  $n = 11$ , EVOO,  $n = 10$ ). (D) Mice were also assessed in the Morris water maze paradigm for the number of entries to the platform zone, the time spent in the platform zone, and the time spent in the NE zone (CTR  $n = 11$ , EVOO,  $n = 10$ ) ( $*P < 0.05$ ). Values represent mean  $\pm$  SEM.

However, during the probe test at 12 month of age (6 months of treatment) we observed that compared with controls, mice receiving the EVOO-diet had a higher number of entries in the platform zone, and spent more time in the platform zone and in the NE zone (Fig. 1D).

### EVOO-rich diet reduces A $\beta$ levels and deposition in 3xTg mice

At 12 months of age, mice were euthanized and brain cortex homogenates assayed for A $\beta$  levels in the RIPA-soluble and formic acid-soluble fractions. Compared with controls, we found that EVOO group presented a decrease in A $\beta$ 1-40 levels that reached the statistical significance only in the formic acid soluble fraction. Although we observed a reduction in the A $\beta$ 1-42 RIPA-soluble and formic acid soluble fractions in brain homogenates from the EVOO-treated mice, in both cases the differences failed to reach statistical significance (Fig. 2A and B). An analysis of the A $\beta$  42/40 ratios for the

RIPA-soluble and formic acid-soluble fractions between the two groups of mice (control/treated) did not show any significant differences (0.25 vs. 0.14 and 0.06 vs. 0.08 respectively). Next, we investigated the effect of EVOO on A $\beta$  deposition by immunohistochemistry. Compared with CTR, we found a statistically significant reduction in the amount of A $\beta$  peptides deposited in the brains of the EVOO-treated animals as measured by 4G8 immunoreactivity (Fig. 2C and D).

To elucidate the possible mechanism responsible for the effect on the A $\beta$  levels and deposition, we assayed the levels of the A $\beta$  precursor protein (APP) and the proteases involved in its metabolism by Western blot. Compared with controls, we found that, EVOO-treated mice had a significant increase in  $\beta$ -secretase (BACE1), sAPP- $\beta$  and  $\alpha$ -secretase (ADAM10) levels (Fig. 2E and F). By contrast, the sAPP- $\alpha$  increased levels failed to reach statistical significance (Fig. 2E and F). No changes were observed in the levels of APP and three of the four components of  $\gamma$ -secretase (i.e., APH1, nicastrin, and Pen2) when the two

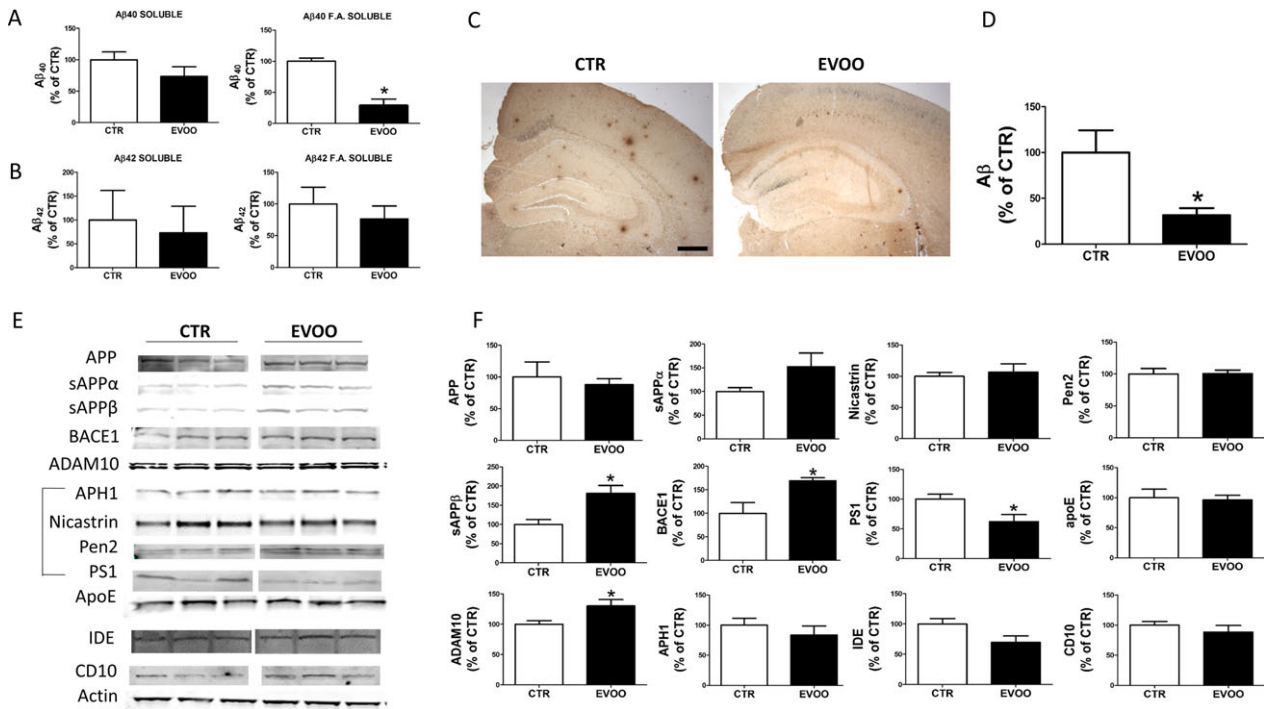


**Figure 2.** Chronic administration of EVOO-rich diet decreases brain A $\beta$  levels and deposition in 3xTg mice. (A,B) RIPA-soluble (RIPA) and formic acid soluble (F.A.) A $\beta$ 1-40 and A $\beta$ 1-42 levels in brain cortex homogenates of 3xTg receiving EVOO ( $n = 8$ ) or vehicle (CTR) ( $n = 8$ ) (C) Representative images of brain sections of 3xTg mice receiving EVOO or vehicle (CTR) immunostained with 4G8 primary antibody (Scale bar 100  $\mu$ m). (D) Quantification of the area occupied by A $\beta$  immunoreactivity in brains of 3xTg mice receiving EVOO ( $n = 4$ ) or vehicle (CTR) ( $n = 4$ ) (\* $P < 0.05$ ). E. Representative Western blots of APP, sAPP $\alpha$ , sAPP $\beta$ , BACE1, ADAM10, APH1, Nicastrin, Pen2, PS1, ApoE, IDE, and CD10 in the brain cortex homogenates from 3xTg mice receiving EVOO ( $n = 4$ ) or vehicle (CTR) ( $n = 4$ ). (F) Densitometric analyses of the immunoreactivities to the antibodies shown in the previous panel (\* $P < 0.05$ ). Values represent mean  $\pm$  SEM.

groups were compared (Fig. 2E and F). Compared with controls, brain homogenates from EVOO-treated mice had a significant increase in the levels of the APP- $\beta$ CTF (Fig. S1). Finally, we looked at some of the proteins that have been involved in A $\beta$  clearance, but no significant differences were found between the two groups in the steady state levels of apolipoprotein E (APOE), neprilysin (CD10), and insulin degrading enzyme (IDE) (Fig. 2E and F).

### EVOO-rich diet attenuates tau pathology

Next, we investigated the effect of EVOO-rich diet consumption on tau phosphorylation and pathology in the brain cortices of the same mice. As shown in Figure 3A, we found a significant reduction in the phosphorylated forms of tau at Ser202/Thr205 and Ser396/Ser404, as recognized by the antibodies AT8 and PHF13, respectively, in the EVOO group when compared with mice on a regular diet. No significant effect of the treatment was observed when the levels of total tau were assessed in the same brain region (Fig. 3A and B). These results were

further confirmed by immunohistochemical analyses (Fig. 3C and D). Since we found changes in tau phosphorylation, next we examined some of the kinases and phosphatases, which are considered major regulators of tau post-translational modifications. As shown in Figure 3E, we did not find any changes between control and EVOO-treated mice in the steady-state levels of P38 MAPK, CDK5 and its two co-activators p35 and p25. By contrast, compared with controls, immunoblot analysis showed a significant decrease in P38 active phosphorylated form (p-P38). Finally, mice fed with EVOO-enriched diet had significantly higher level of protein phosphatase 2A (PP2A) (Fig. 3E and F).

### EVOO-rich diet improves synapse integrity and neuroinflammation

To assess whether the improved cognitive performance and AD pathology seen in the EVOO-treated mice was also biochemically characterized by an amelioration of synaptic integrity, we assayed the steady state levels of two major synaptic proteins: synaptophysin (SYN) indices

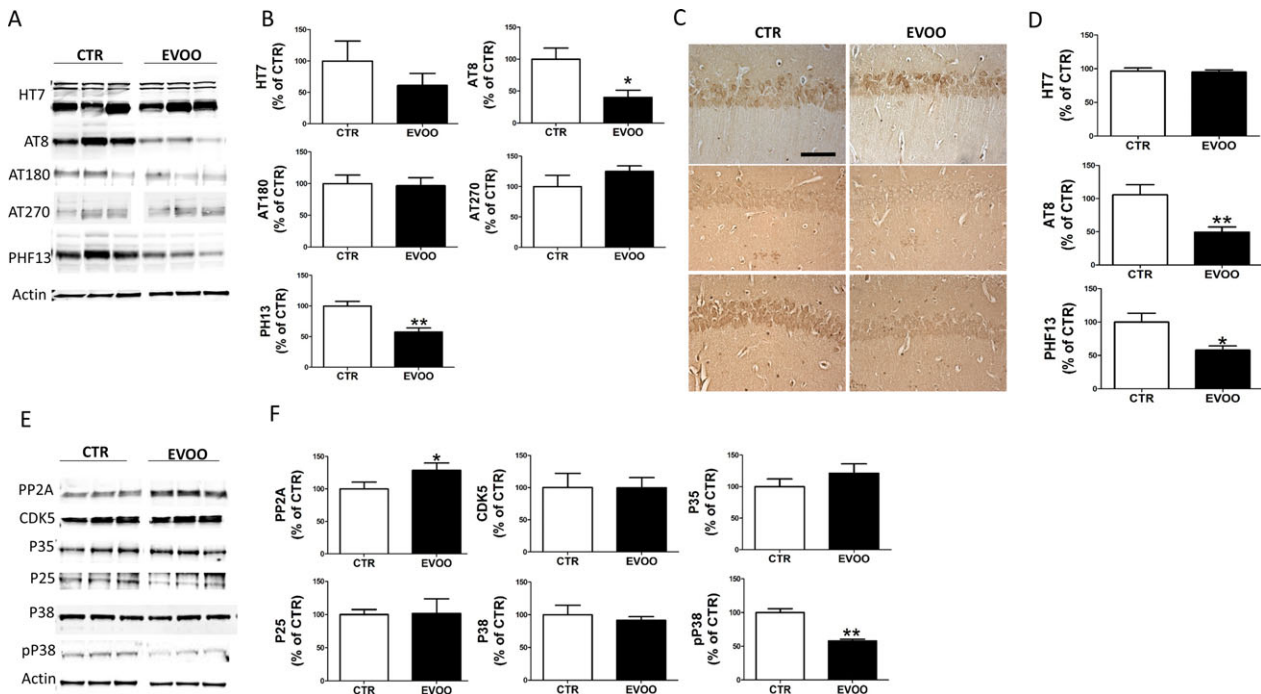


**Figure 3.** Chronic administration of EVOO-rich diet reduces tau neuropathology in 3xTg mice. (A) Representative Western blots of total soluble tau (HT7), phosphorylated tau at residues ser202/thr205 (AT8), thr231/ser235 (AT180), and thr181 (AT270), and ser396 (PHF13) in brain cortex homogenates from 3xTg mice receiving EVOO ( $n = 6$ ) or vehicle (CTR) ( $n = 6$ ). (B) Densitometric analyses of the immunoreactivities to the antibodies shown in the previous panel (\* $P < 0.05$ , \*\* $P < 0.01$ ). (C) Representative images of brain sections from 3xTg mice receiving EVOO or vehicle (CTR) immunostained with HT7, AT8 and PHF13 antibodies. (D) Quantification of the integrated optical density (IOD) by the immunoreactivity to the same antibodies shown in the previous panel (\* $P < 0.05$ , \* $P < 0.01$ ). (E) Representative Western blot analysis of PP2A, CDK5, P35, P25, P38 and pP38 in brain cortex homogenates from 3xTg mice receiving EVOO ( $n = 4$ ) or vehicle (CTR) ( $n = 4$ ). (F) Densitometric analyses of the immunoreactivities to the antibodies shown in the previous panel; (\*\* $P < 0.01$ ). Values represent mean  $\pm$  SEM.

of presynaptic integrity, and the postsynaptic density protein 95 (PSD95). As shown in Figure 4A, no differences were observed between the two groups when PSD95 levels were measured. By contrast, mice fed with EVOO-rich diet when compared with the control group, displayed a statistically significant increase in the steady state levels of SYP. Confirming the immunoblot data, EVOO-treated mice showed a significant increase in brain immunoreactivity for SYP (Fig. 4C and D). In addition, we observed that compared with controls, mice receiving the EVOO-rich diet had a significant reduction in the steady state levels of IBA1, a marker of microglia activation, which was also confirmed by immunohistochemistry (Fig. 4 E and F). By contrast, no differences between the two groups were found when GFAP levels, marker of astrocytes activation, were assayed (Fig. 4E and F).

### EVOO-rich diet does not affect CREB signaling on 3xTg mice

Since CREB and CREB-regulated proteins have been previously reported to be altered in AD pathology, next we

investigated the effect of our EVOO-rich diet on total CREB levels and its phosphorylated form at Ser133 (p-CREB). As shown in Figure 5, the levels of total CREB and p-CREB were not changed in the brain of EVOO-treated mice compared to controls. Additionally, no differences were detected in the protein expression level of BDNF and cFos, two important CREB target genes, between the two groups (Fig. 5A and B).

### EVOO-rich diet induces autophagy in 3xTg mice

Since we observed that chronic administration of EVOO-rich diet resulted in a marked reduction in  $A\beta$  deposition but we did not find differences in the  $A\beta$  degrading enzymes (i.e., IDE, ApoE and CD10), we looked at several autophagy markers. Among them, we assessed ATG5-12, ATG7 and the microtubule-associated protein light chain 3 conversion (LC3I/II) which are considered essential for the autophagosome formation and autophagic flux, respectively.<sup>17,18</sup> As shown in Figure 5C, ATG5 and ATG7 immunoreactivity was significantly stronger in

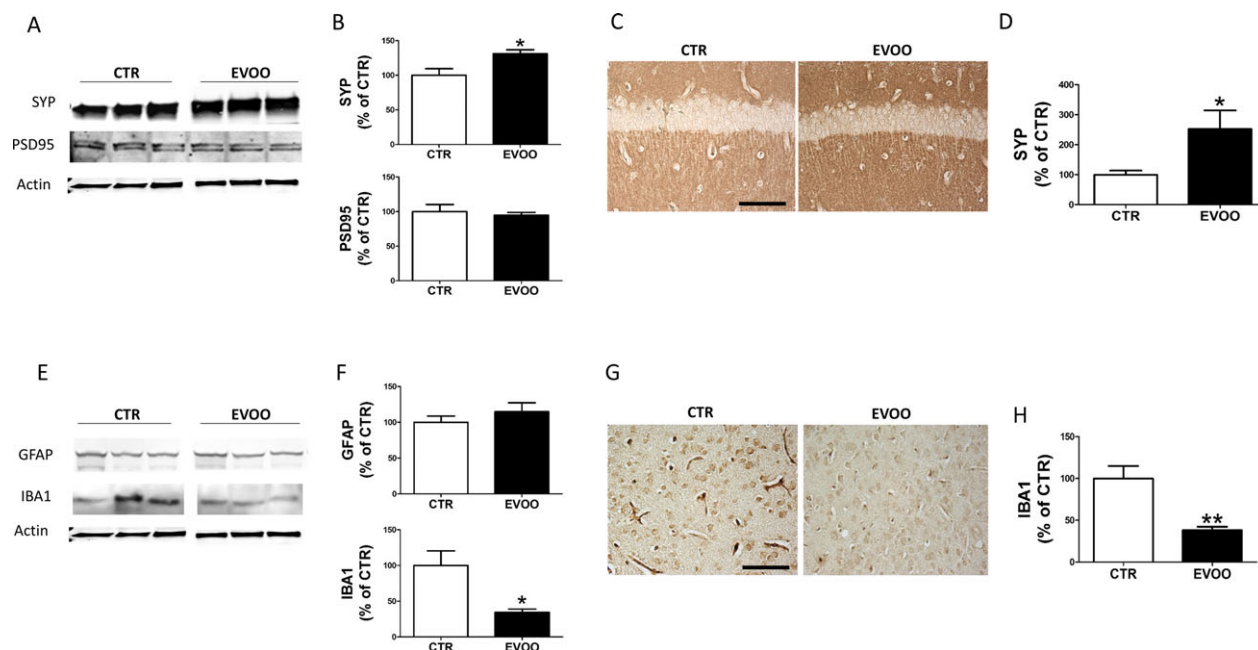


**Figure 4.** Effect of chronic administration of EVOO-rich diet on synaptic integrity and neuroinflammation. (A) Representative western blot analyses of synaptophysin (SYP) and postsynaptic density protein 95 (PSD95) in brain cortex homogenates of 3xTg mice treated with EVOO ( $n = 4$ ) or vehicle (CTR) ( $n = 4$ ). (B) Densitometric analyses of the immunoreactivities to the antibodies shown in the previous panel ( $*P < 0.05$ ). (C) Representative images of brain sections from 3xTg mice receiving EVOO or vehicle (CTR) immunostained with SYP antibody. (D) Quantification of the integrated optical density (IOD) by the immunoreactivity to the same antibody shown in the previous panel ( $*P < 0.05$ ). (E) Representative western blot analyses of GFAP and IBA1 in brain cortex homogenates of 3xTg mice treated with EVOO ( $n = 4$ ) or vehicle (CTR) ( $n = 4$ ). (F) Densitometric analyses of the immunoreactivities to the antibodies shown in the previous panel ( $*P < 0.05$ ). (G) Representative images of brain sections from 3xTg mice receiving EVOO or vehicle (CTR) immunostained with IBA1 antibody. (H) Quantification of the integrated optical density (IOD) by the immunoreactivity to the same antibody shown in the previous panel ( $**P < 0.01$ ). Values represent mean  $\pm$  SEM.

EVOO-treated mice compared to controls suggesting induction of autophagy in this group of 3xTg mice. On the other hand, LC3I/II conversion ratio was not significantly different changes when the two groups of mice were compared (Fig. 5C and D).

## Discussion

The data presented in the current paper demonstrate that chronic administration of a diet enriched with EVOO results in an amelioration of working memory, spatial learning, and synaptic pathology, a significant reduction in the amount and deposition of  $A\beta$  peptides, and a decrease in the tau neuropathology secondary to an activation of autophagy.

Taken together our findings provide strong experimental support for the translational value of EVOO as a therapeutic tool with potential disease-modifying activity for AD since it beneficially influenced all three major aspects of the AD phenotype in the implemented disease model.

Increasing evidence has been accumulated showing that chronic exposure to the Mediterranean diet associates

with a lower risk of AD and cognitive impairments.<sup>19,20</sup> The diet was originally described in studies focusing on food intake in countries of the Mediterranean area such as Italy and Greece, and its relationship with rates of chronic diseases and life expectancy. It soon became apparent that this specific diet was associated with longer life expectancy and lower rates of cardiovascular diseases and dementias than the ones observed in populations exposed to other diets.<sup>21</sup> Thus, the results of several cross-sectional investigations have been mainly consistent showing positive outcomes. Among the key elements of the Mediterranean diet, an important role has been attributed to daily intake of fresh fruit and vegetable, cereals, beans, and legumes and the usage of EVOO as a primary source of fat.<sup>22</sup> In particular, average daily consumption of 30–50 mL per day of EVOO has been suggested as the most important and integral component of the diet<sup>23,24</sup> resulting in the common idea that EVOO plays a major role in the health benefit of this diet.

Previous *in vitro* studies have shown that EVOO positively modulates cell membrane structure in response to free-radical dependent oxidative stress.<sup>25</sup> Others have demonstrated that EVOO has direct antioxidant property

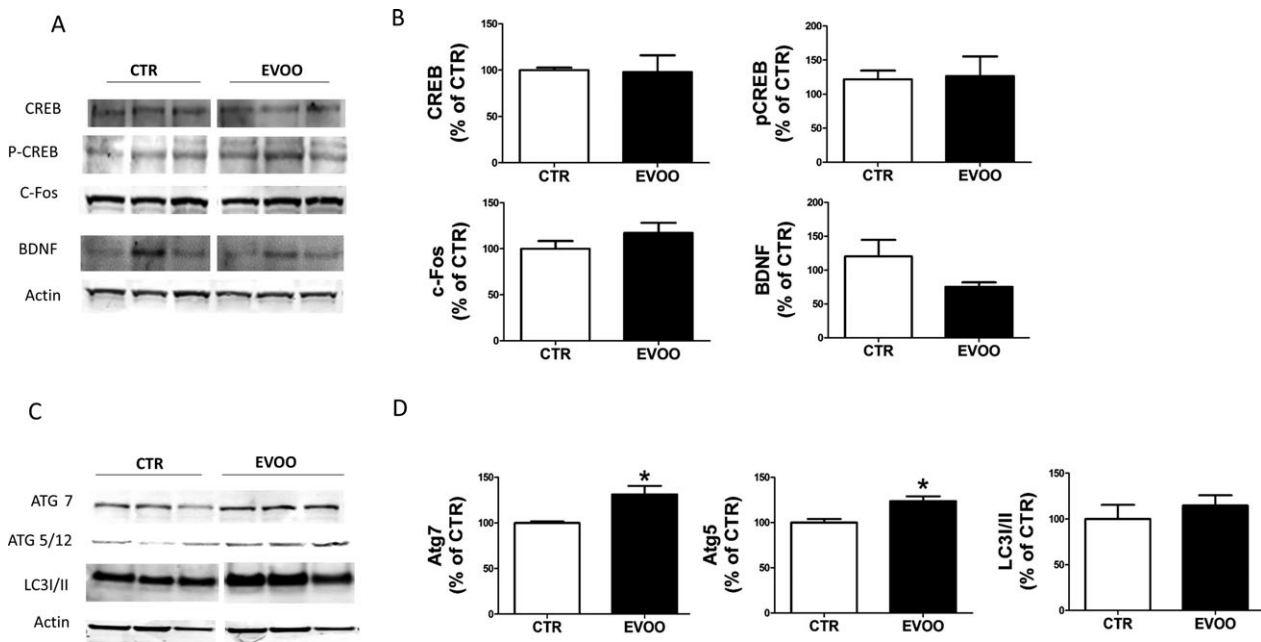


**Figure 5.** Effect of chronic administration of EVOO-rich diet on autophagy. (A) Representative Western blot analyses of CREB, p-CREB, c-Fos, BDNF, in brain cortex homogenates of 3xTg mice receiving vehicle (CTR) or EVOO. (B) Densitometric analyses of the immunoreactivities to the antibodies shown in the previous panel. (C) Representative Western blot analyses of ATG7, ATG5/12 and LC3/II in brain cortex homogenates of 3xTg mice receiving vehicle (CTR) or EVOO. (D) Densitometric analyses of the immunoreactivities to the antibodies shown in the previous panel (\* $P < 0.05$ ) ( $n = 5$ ,  $n = 5$ ). Values represent mean  $\pm$  SEM.

by acting as scavenger of reactive oxygen species and blocker of free radical formation in cellular system.<sup>26</sup> On the other hand, animal model studies have provided evidence for a beneficial effect of EVOO on behavior as well as brain amyloidosis.<sup>27</sup> However, since these models do not develop the second most important hallmark lesion of the AD brain pathology, it remains to be investigated whether or not EVOO has a beneficial effect on the development of tau neuropathology.

To address this scientific question, we utilized a different mouse model, the 3xTg, which by contrast with the ones implemented previously in addition to  $A\beta$  plaques develop AD-like tau neurofibrillary tangle pathology. First, compared with 3xTg kept on a regular chow diet, the ones receiving EVOO-supplemented diet had a significant improvement in the percentage of spontaneous alternations in the Y-maze, a paradigm, which assesses rodent working memory.<sup>28</sup> Importantly, no significant differences were observed between the two groups when the number of entries in each arm of the maze was considered suggesting that the diet did not alter the motor ability of the mice.

In addition, we observed that the same mice performed better the probe test, which measures their spatial learning and memory ability. Supporting the beneficial effect on the behavior responses, we found that the same mice had biochemical evidence for a reduction in synaptic

pathology as demonstrated by the higher levels of synaptophysin, a well-established presynaptic marker, in the brains of EVOO-treated mice.

Consistent with the behavioral results, and confirming previous observation, we found that mice receiving EVOO-rich diet had a reduction in the formic acid-soluble fraction of the  $A\beta$ 1-40. This was associated with a significant decrease in the  $A\beta$  immunoreactivity in the cortex and hippocampus brain regions of the same mice suggesting that  $A\beta$  deposition was significantly affected in the EVOO treated group. When we assessed the proteolytic enzymes and pathways involved in the APP metabolism differently from another report we observed that compared with controls, the treated mice had an increase in  $\alpha$ -secretase and  $\beta$ -secretase and their products, s-APP $\alpha$  and the sAPP $\beta$ .<sup>11</sup> While that study does not provide data on these two proteases, we think that the discrepancy in the result for the sAPP $\beta$  could be secondary to the different mouse model implemented by the authors.<sup>11</sup> Moreover, by contrast with other reports, we were not able to show any effect of the EVOO on some of the major protein systems in place to control  $A\beta$  clearance and degradation.<sup>29</sup> Thus, steady state levels of apoE, a major  $A\beta$  chaperone, levels of neprilysin and IDE, two major  $A\beta$  catabolic pathways, were no different between the controls and EVOO-treated mice.

Here, we show for the first time that chronic supplementation of EVOO-rich diet results in a modulation of tau metabolism. By using both biochemistry and immunohistochemistry approaches, we found that 3xTg mice receiving the diet containing EVOO had a significant reduction in tau phosphorylation. This decrease was selective, because it was observed only at Ser202/Thr205 (as recognized by the antibody AT8), and at Ser396 (as recognized by the antibody PHF13), but not at other tau epitopes. By contrast, no effect of EVOO was observed when we assayed the level of total soluble tau protein. To determine the molecular mechanism responsible for the reduced tau phosphorylation, next we assessed the levels of some of the kinases and phosphatases which have been considered major players in tau post-transcriptional modifications. In our study, we found that while the cdk5 pathway was not different between the two groups, mice receiving EVOO-rich diet had a significant reduction in the phosphorylated form of the p38 kinase, and a significant elevation of the steady state levels of phosphatase PP2A.

Aside from A $\beta$ , tau and synaptic pathology, activation of microglia and astrocytes is another important feature found consistently in the AD brain, and some work even suggests that these cells play a functional role in AD pathogenesis.<sup>30</sup> Interestingly, in our study we found that the expression levels of IBA1, a marker of microglia activation, was significantly reduced in the EVOO-treated mice.

Based on the observation that EVOO treated mice had a reduction in the insoluble forms of A $\beta$  and in the pro-aggregatory highly phosphorylated isoforms of tau protein, we hypothesized a potential involvement of the cellular clearing system as the mechanism responsible for the biological effect. For this reason, next we assessed several markers of autophagy activation in the brain of the two groups of mice. Consistent with our hypothesis, we noted that compared with controls, brains from EVOO-treated mice had a significant increase in the steady state levels of ATG5 and ATG7, which are established biomarkers of autophagy activation. Interestingly our conclusion is in agreement with previous observations showing that oleochemical, a major component of EVOO, can act as an activator of autophagy.<sup>31</sup>

In conclusion, our investigation establishes for the first time to the best of our knowledge a protective effect of EVOO in modulating tau phosphorylation, memory impairments, synaptic integrity, and neuroinflammation in a mouse model of AD with plaques and tangles.

The translational value of our findings lies in the observation that EVOO supplementation can influence the entire spectrum of the AD phenotype. Our studies provide mechanistic support to the positive cross-sectional

and longitudinal data on this component of the Mediterranean diet, and most importantly the biological rationale to the novel hypothesis that EVOO could be considered as a viable therapeutic opportunity for preventing or halting AD.

## Acknowledgment

This work presented in this paper was in part supported by a grant from the Wanda Simone Endowment for Neuroscience.

## Conflict of Interest

The authors declare no conflict of interest.

## References

1. Alzheimer's Association. Alzheimer's disease facts and figures. *Alzheimer Dement* 2016;2016:459–509.
2. Giannopoulos PG, Praticò D. Alzheimer's disease In: C. R. Martin and V. Reddy, eds. *Diet and Nutrition in Dementia and Cognitive Decline*. pp. 13–21. London: Elsevier, 2015.
3. Hurd MD, Martorelli P, Langa KM. Monetary cost of dementia in the United States. *N Engl J Med* 2013;369:489–490.
4. Safouris A, Tsivgoulis G, Sergentanis TN, Psaltopoulou T. Mediterranean diet and risk of dementia. *Curr Alzheimer Res* 2015;12:736–744.
5. Singh B, Parsaik AK, Mielke MM, et al. Association of Mediterranean diet with mild cognitive impairment and Alzheimer's disease: a systematic review and meta-analysis. *J Alzheimer's Dis* 2014;39:271–282.
6. Tuck K, Hayball PJ. Major phenolic compounds in olive oil: metabolism and health effects. *J Nutr Biochem* 2002;13:636–644.
7. Salvini S, Sera F, Caruso D, et al. Daily consumption of a high-phenol extra virgin olive oil reduces oxidative DNA damage in post-menopausal women. *Br J Nutr* 2006;95:742–751.
8. Farr SA, Price TO, Dominguez LJ, et al. Extra virgin olive oil improves learning and memory in SAMP8 mice. *J Alzheimer's Dis* 2012;28:81–92.
9. Pitozzi V, Jacomelli M, Zaid M, et al. Effects of dietary extra virgin olive oil on behavior and brain biochemical parameters in ageing rats. *Br J Nutr* 2010;103:1674–1683.
10. Pitozzi V, Jacomelli M, Catelan D, et al. Long-term extra virgin olive oil rich in polyphenols reverses age-related dysfunctions in motor coordination and contextual memory in mice: role of oxidative stress. *Rejuvenation Res* 2012;15:601–612.
11. Qosa H, Mohamed LA, Bataresh YS, et al. Extra virgin olive oil attenuates amyloid- $\beta$  and tau pathologies in the

- brains of TgSwDI mice. *J Nutr Biochem* 2015;26:1479–1490.
12. Oddo S, Caccamo A, Shepherd JD, et al. Triple transgenic model of Alzheimer's disease with plaques and tangles: intracellular Abeta and synaptic dysfunction. *Neuron* 2003;39:409–421.
  13. Li J-G, Barrero C, Merali S, Praticò D. Five lipoxygenase hypomethylation mediates the homocysteine effect on Alzheimer's phenotype. *Sci Rep* 2017;7:46002.
  14. Lauretti E, Li J-G, Di Meco A, Praticò D. Glucose deficit triggers tau pathology and synaptic dysfunction in a tauopathy mouse model. *Transl Psychiat* 2017;7:e1020.
  15. Giannopoulos PF, Chu J, Sperow M, et al. Pharmacologic inhibition of 5-lipoxygenase improves memory, rescues synaptic dysfunction, and ameliorates tau pathology in a transgenic model of tauopathy. *Biol Psychiatry* 2015;78:693–701.
  16. Joshi YB, Giannopoulos PF, Chu J, et al. Absence of ALOX5 gene prevents stress-induced memory deficits, synaptic dysfunction and tauopathy in a mouse model of Alzheimer's disease. *Hum Mol Genet* 2014;23:6894–6902.
  17. Jin M, Klionsky DJ. The core molecular machinery of autophagosome formation. *Autophagy Cancer* 2013;8:25–45.
  18. Mizushima N, Yoshimori T, Levine B. Methods in mammalian autophagy research. *Cell* 2010;140:313–326.
  19. Wu L, Sun D. Adherence to Mediterranean diet and risk of developing cognitive disorders: An updated systematic review and meta-analysis of prospective cohort studies. *Sci Rep* 2017;23:41317.
  20. Peterson SD, Philippou E. Mediterranean diet, cognitive function, and dementia: a systematic review of the evidence. *Adv Nutr* 2016;7:889–904.
  21. Feart C, Samieri C, Alles B, Barberger-Gateau P. Potential benefits of adherence to the Mediterranean diet on cognitive health. *Proc Nutr Soc* 2013;72:140–152.
  22. Guasch-Ferré M, Hu FB, Martínez-González MA, et al. Olive oil intake and risk of cardiovascular disease and mortality in the PREDIMED Study. *BMC Med* 2014;140–152.
  23. Corona G, Spencer JP, Dessi MA. Extra virgin olive oil phenolics: absorption, metabolism, and biological activities in the GI tract. *Toxicol Ind Health* 2009;25:285–293.
  24. Vissers MN, Zock PL, Katan MB. Bioavailability and antioxidant effects of olive oil phenols in humans: a review. *Eur J Clin Nutr* 2004;58:955–965.
  25. Lopez S, Bermudez B, Montserrat-de la Paz S, et al. Membrane composition and dynamic: a target of bioactive virgin olive oil constituents. *Biochim Biophys Acta* 2014;1838:1356–1638.
  26. Aparicio-Soto M, Sánchez-Hidalgo M, Cárdeno A, et al. Dietary extra virgin olive oil attenuates kidney injury in pristane-induced SLE model via activation of HO-1/Nrf-2 antioxidant pathway and suppression of JAK/STAT, NF- $\kappa$ B and MAPK activation. *J Nutr Biochem* 2016;27:278–288.
  27. Abuznait AH, Qosa H, Busnena B, et al. Olive-oil-derived oleocanthal enhances b-amyloid clearance as a potential neuroprotective mechanism against Alzheimer's disease: in vitro and in vivo studies. *ACS Chem Neurosci* 2013;4:973–982.
  28. Lauretti E, Di Meco A, Chu J, Praticò D. Modulation of AD neuropathology and memory impairments by the Isoprostane F2 alpha is mediated by the thromboxane receptor. *Neurobiol Aging* 2015;36:812–820.
  29. Leissring MA. A $\beta$ -degrading proteases: therapeutic potential in alzheimer disease. *CNS Drugs* 2016;30:667–675.
  30. Joshi YB, Praticò D. Neuroinflammation and Alzheimer's disease: lessons learned from 5-Lipoxygenase. *Translational Neurosci* 2014;5:197.
  31. Oliván S, Martínez-Beamonte R, Calvo AC, et al. Extra virgin olive oil intake delays the development of amyotrophic lateral sclerosis associated with reduced reticulum stress and autophagy in muscle of SOD1G93A mice. *J Nutr Biochem* 2014;25:885–892.

## Supporting Information

Additional Supporting Information may be found online in the supporting information tab for this article:

**Figure S1.** (A) Representative Western blot analysis for APP $\beta$ -CTF (C-99) in the brain cortex homogenates from 3xTg mice receiving vehicle (CTR) ( $n = 5$ ) or EVOO-rich diet ( $n = 5$ ). (B) Densitometric analyses of the immunoreactivity to the antibody shown in the previous panel (\*\* $P < 0.01$ ). Values represent mean  $\pm$  SEM.